JAFIB®

Original Research

Journal of Atrial Fibrillation

www. jafib.com

Mechanistic Insights Into Durable Pulmonary Vein Isolation Achieved By Second-Generation Cryoballoon Ablation

Yasuo Okumura, Ichiro Watanabe, Kazuki Iso, Keiko Takahashi, Koichi Nagashima, Kazumasa Sonoda, Hiroaki Mano, Naoko Yamaguchi, Rikitake Kogawa, Ryuta Watanabe, Masaru Arai, Kimie Ohkubo, Sayaka Kurokawa, Toshiko Nakai, Atsushi Hirayama

Division of Cardiology, Department of Medicine, Nihon University School of Medicine, Tokyo, Japan.

Abstract

Background: The mechanism explaining the efficacy of cryoballoon ablation (CBA) for atrial fibrillation has not been clarified.

Methods and Results: We compared lesion characteristics between patients in whom pulmonary vein isolation (PVI) was performed by CBA (n=56) and those by contact force (CF)-based RF ablation (n=56). We evaluated the 3-dimensional PV morphology before and after cryoballoon inflation. After PVI, a 3D left atrial voltage map was created. Pacing (10 mA and 2 ms) was performed within the low voltage area from the ablation line, and electrically unexcitable ablated tissue was identified. ATP-provoked dormant conduction after PVI occurred in 9 of the 224 (4%) PVs in the CBA group and in 13 of the 224 (6%) PVs in the CF group (P=0.3935). The inflated balloon stretched the PV from the original PV ostial surface by 5.2±3.3 mm, but at sites with (vs, sites without) residual PV potential/dormant conduction, the extent of the PV distension was reduced (2.6±3.4 mm vs. 5.3±3.3 mm, P<0.0001). The unexcitable ablated tissue around the PVs was significantly wider in CB patients than in CF patients (16.7±5.1 mm vs. 5.3±2.3 mm, P<0.0001).

Conclusions: Use of the cryoballoon significantly distends the PV. Without this extensive distention, PVI may not be successful. CBA seems to yield wide unexcitable ablation zones. These factors seem to explain the durability of CBA lesions.

Introduction

Cryothermal energy has emerged as an alternative ablation energy that does not issue in the clot formation and excessive tissue damage that occur with radiofrequency (RF) energy-based catheter ablation.[1] Although cryothermal energy is a milder and safer form of energy than RF energy, pulmonary vein isolation (PVI) performed with a second-generation cryoballoon has been highly successful in cases of paroxysmal atrial fibrillation (AF) and comparable to PVI performed by point by point-based RF ablation[2]–[6] or even contact force (CF)-based RF ablation.[7],[8] Despite the efficacy of cryoballoon ablation (CBA), however, some patients suffer recurrence of the AF, due mainly to PV reconnections or to non-PV triggers.[9],[10] Thus far, the mechanisms explaining durable and non-durable lesion formation around the PV ostium by means of second-generation CBA have not been fully investigated. Because establishing good balloon surface-to-tissue contact is essential for successful CBA of AF, we investigated, by means of 3-dimensional (3D) geometric imaging, how the inflated balloon surface contacts the 4 PVs. We then characterized lesions created around the PV ostia by CBA and those created by CF-based ablation to clarify the mechanism responsible for the efficacy of CBA.

Key Words

atrial fibrillation, cryoballoon ablation, pulmonary vein isolation, pulmonary vein distension.

Corresponding Author

Yasuo Okumura, MD Division of Cardiology, Department of Medicine,
Nihon University School of Medicine Ohyaguchi-kamicho, Itabashi-ku,
Tokyo 173-8610,
Japan Tel: +81-3-3972-8111
Fax: +81-3-3972-1098
E-mail: yasuwo128@yahoo.co.jp

Material and Methods

Study Patients

The study involved 112 consecutive patients treated for AF (symptomatic paroxysmal AF [n=88] or persistent AF [n=24]) at Nihon University Itabashi Hospital between September 2014 and December 2015. The patient series comprised 72 men and 40 women with a mean±SD age of 63.8±7.7 years and median duration of AF of 18 months (interquartile range, 6–48 months). Patients were blindly (but not randomly) assigned to 1 of 2 ablation procedures: PVI performed by means of second-generation CBA (CBA group, n=56) and PVI performed by means of CF-based RF catheter ablation (CF group, n=56). Written informed consent was obtained from all patients. All antiarrhythmic drugs were withdrawn for at least 5 half-lives prior to the procedure. Transesophageal and transthoracic echocardiography were performed 1 day before the ablation procedure with an ACUSON Sequoia C256 echocardiography system (Siemens Medical Solutions USA, Inc., Malvern, PA). LA diameter (LAD) and maximum LA volume (by the prolate ellipsoid method) were determined, and the left ventricular ejection fraction (LVEF) was determined by means of M-mode echocardiography (Teichholz method). Multi-slice computed tomography was performed with a 320-detector row, dynamic volume scanner (Aquilion ONE; Toshiba Medical Systems, Tokyo, Japan) in all patients for 3D reconstruction of the left atrium (LA) and PVs before ablation.

Electrophysiologic Study and Ablation

Electrophysiologic study was performed in all patients under conscious sedation achieved with dexmedetomidine and fentanyl.

After vascular access was obtained, single transseptal puncture was performed, and intravenous heparin was administered to maintain an activated clotting time of >300 seconds.[11],[12]

CBA

In all patients who underwent CBA, 2 SL0 long sheaths (St. Jude Medical, Inc., St. Paul, MN, USA) were inserted into the LA via the puncture hole.[11] The 3D geometry of the LA and PVs was reconstructed with an EnSite NavX mapping system (St. Jude Medical) from data obtained with a 20-pole circular mapping catheter (4-mm interelectrode spacing; Inquiry AFocus II EB catheter; St. Jude Medical) or a 10-pole mapping catheter with 5-mm interelectrode spacing (Snake, Japan Lifeline, Inc., Tokyo, Japan) through 1 of the 2 SL0 sheaths. An exchange length (0.035 inch) guidewire was introduced into the left superior (LS) PV, over which another SL0 sheath was exchanged for a 15Fr deflectable sheath (Flexcath, Medtronic, Inc., Minneapolis, MN, USA). An Artic Front Advance 28-mm cyroballoon (CB-Adv) (Medtronic) with an Achieve inner lumen mapping catheter was placed in the LA through the steerable 15Fr sheath. The CB-Adv was then inflated and advanced successively to each PV ostium to establish optimal PV occlusion, determined by the absence of contrast leakage. To avoid a vigorous wedging of the balloon inside the PVs, we used the — proximal-seal| technique for all RSPV and LSPV, i.e., withdrawing the inflated cryoballoon until a small leak was observed and then performing a small repositioning of the cryoballoon were applied.[13] Cryoenergy was delivered to each PV after occlusion was established. Ablation of each PV antrum was performed with a 180-s application followed by a 120-s or 180-s application. Continuous monitoring of the phrenic nerve during ablation of the right superior and inferior PVs (RSPV and RIPV, respectively) was systematically performed by pacing the right phrenic nerve from the superior vena cava.[11] After each CBA procedure, PVI was confirmed with the 20-pole circular mapping catheter. If residual PV potentials were revealed, additional cryoenergy was delivered.

CF-Based RF Ablation

In all patients who underwent CF-based ablation, extensive encircling ipsilateral PVI was performed, guided by a double Lasso catheter and the 3D geometric map reconstructed with the CARTO mapping system (Biosense Webster, Inc., Diamond Bar, CA), as previously reported.[12] The point-by-point ablation method was used by a CF-sensing irrigated tip catheter with 2-5-2 mm spacing (Thermocool Smart Touch; Biosense Webster) under VisiTag system guidance.[12] RF energy was delivered at a maximum power output of 25–30 W and a target CF of 10–20 grams with a force-time integral of > 400 gs. The upper temperature limit was set to 43°C at a saline irrigation rate of 17–30 mL/min (CoolFlow Pump; Biosense Webster). PVI was confirmed with the Lasso catheters. If the PV remained connected, additional touch-up CF-guided ablation lesions were created until PVI was achieved.

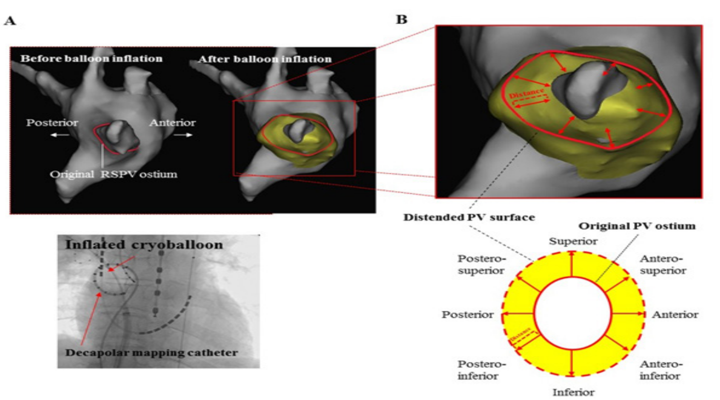

Figure 1: Representative 3D maps created with the use of a mapping catheter before and after inflation of the cryoballoon. The example here is of the RSPV ostium (A). Maps were used to measure the extent of PV distension (B). After inflation of a 28-mm cryoballoon, we maneuvered the decapolar mapping catheter around the balloon, fluoroscopically verifying contact between the balloon and the PV (A, lower panel). 3D, 3 dimensional; PV, pulmonary vein; RSPV, right superior PV.

Creation of 3D Images of the PV Ostium After Inflation of the Cyoballoon

For 21 of the 56 patients who underwent CBA, we created 3D images of the distended PV ostium after inflating the cyoballoon. Upon completion of the CBA procedure, the Snake mapping catheter was advanced into the LA through the SL0 sheath. The balloon was again inflated, and we created the 3D geometry of the distended PV by carefully manipulating the mapping catheter around the inflated balloon surface, which was now in contact with the endocardium at the target PV ostium [Figure 1]. To minimize distortion by the mapping catheter, we created the 3D geometric image of the expanded PV surface during pullback of the mapping catheter, which we performed in a step-by-step manner from different directions.[14] At each PV, we measured the amount of balloon-induced distention at the PV ostium by measuring the distance between the original PV surface and the surface of the distended PV at the 8 segments: the superior, antero-superior, anterior, antero-inferior, inferior, postero-inferior, posterior, and postero-superior segments [Figure 1]. Finally, we excluded the diameter (2mm) of the tip of the mapping catheter from the distance between the original PV surface and surface of the distended PV, and used that distance for the analysis, because

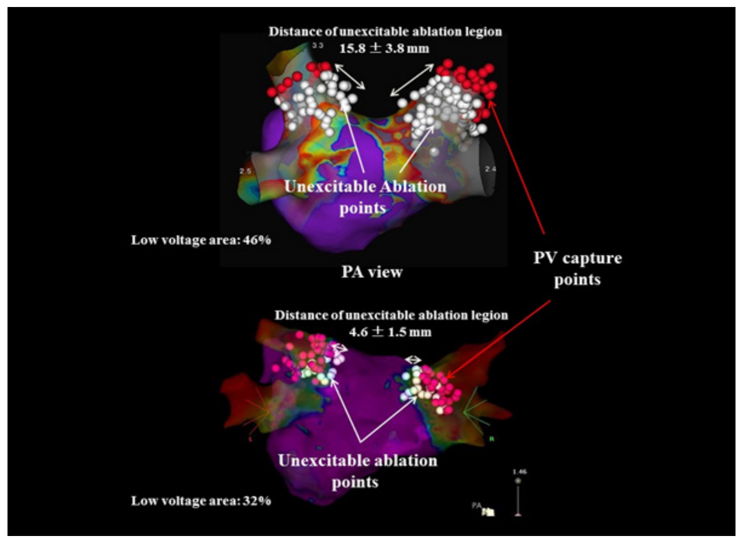

Figure 2: Assessment of low voltage areas and unexcitable ablation lesions around the PV ostium created by CBA and CF-guided radiofrequency catheter ablation. Shown are low voltage maps after CBA (upper panel) and after CF-guided ablation (lower panel) (A). The low voltage area was slightly larger after CBA than after CF-guided ablation. The width of unexcitable tissue along the ablation line was significantly wider after CBA than after CF-guided ablation (B). White dots indicate absence of capture, and red dots indicate capture within the low voltage zone of the ablated PV ostium. CBA, cryoballoon ablation; CF, contact force; PV, pulmonary vein.

the catheter tip further distended the ostia beyond that of the CB by 2mm.

Identification and Measurement of Low Voltage Areas and Unexcitable Scar Tissue

For each patient, after complete CF-based PVI or completion of 2 (or 3) cryoenergy applications at each PV, a 3D LA voltage map was created, and the percentage of the low voltage area (<0.5 mV), i.e., the ratio of the low voltage area to the total PV-LA surface area (defined by the surface area of the total LA and the distal segments of the PVs 10 mm from each PV ostium) was calculated. After placement of the circular mapping catheter distally within the PV, pacing (10 mA, 2 ms) was performed by the ablation catheter (or the mapping catheter) with 2-mm interelectrode spacing within the low voltage area from the ablation line to the distal segments of the PVs, and we identified whether pacing captured the distal PV tissues or not by the circular mapping catheter. Electrically unexcitable regions were defined as sites where there was no pace capture [Figure 2]. We measured the distance from the edge of the low voltage area to

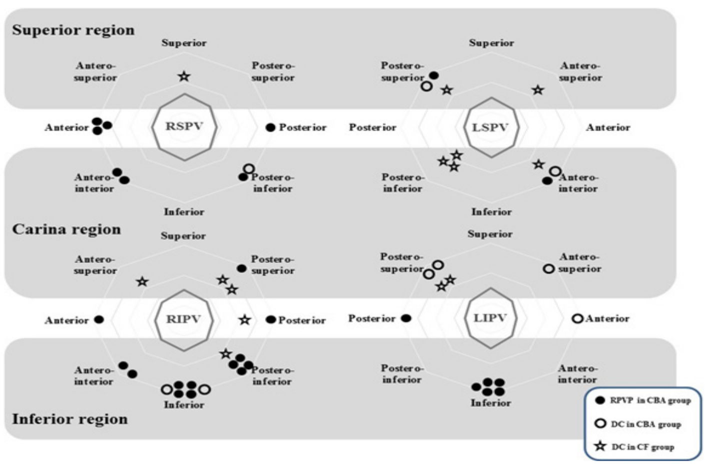

Figure 3: Location of residual PV potentials and dormant conduction provoked by ATP after CBA and CF-guided radiofrequency ablation. RSPV, right superior PV; RIPV, right inferior PV; LSPV, left superior PV; LIPV, left inferior PV; CBA, cryoballoon ablation; CF, contact force; PV, pulmonary vein.

the center of the tag at the unexcitable region in each of the PV segments (except the inferior segment) shown in [Figure 2]. We did not include the RIPV or left inferior (LI) PV because of the difficulty in identifying sites of capture within the short sleeve of each of these PVs.

Ensuring Complete PVI

In patients who underwent CBA, if residual PV potentials around the PV antrum were identified on the 3D LA voltage maps and Lasso catheter recordings despite a total of 3 cryoenergy applications, touch-up RF ablation was performed at acute PV conduction sites with a 4-mm irrigated tip Safire BLU Duo ablation catheter with 2-5-2 mm spacing (St. Jude Medical).

In all patients, 30 minutes after PVI, adenosine triphosphate (ATP) (30 mg) was administered intravenously by bolus injection to provoke dormant PV conduction.[12] Sites of dormant PV conduction were verified with the circular mapping catheter. Sites of residual PV potential and/or breakthrough sites, i.e., sites of dormant PV conduction, were categorized according to the PV segment in which they were revealed. RF energy was applied to the conduction gaps until the dormant PV conduction disappeared. Cavo-tricuspid isthmus ablation was performed when typical atrial flutter was induced by burst atrial pacing or observed clinically.

Post-Ablation Follow-Up

All patients' antiarrhythmic drugs were resumed after the procedure but then stopped after a 3-month post-ablation blanking period. All underwent routine follow-up examinations at our outpatient clinic 2 weeks after ablation, 1 month after ablation, and at 1-to-3-month intervals thereafter for at least 6 months. Twenty-four-hour Holter monitoring was scheduled between 3 and 6 months after ablation. An ECG event recorder was used if a patient reported cardiac symptoms. All documented AF episodes of >30-s duration on the standard ECG, ECG event monitor, or 24-hour Holter recording were considered a recurrence.

Statistical Analysis

Continuous variables are expressed as mean±SD or median values and interquartile ranges. Differences in continuous variables between the CBA group and CF group were analyzed by unpaired t-test or Mann-Whitney U-test, as appropriate. Differences in the extent of distention between the 4 PVs and between PV segments were examined by analysis of variance (ANOVA). Differences in categorical variables were analyzed by chi-square test. P <0.05 was accepted as statistically significant. All statistical analyses were performed with JMP 10 software (SAS Institute, Cary, NC).

Results

Patient and Procedural Characteristics

Patient characteristics and transthoracic echocardiographic variables are summarized per group in [Table 1]. There was no significant difference in clinical characteristics, LAD, or LVEF between the CBA group and the CF group.

Residual PV Potentials After CBA and Dormant PV Conduction Provoked by ATP

A total of 2.2±0.8 cryoenergy applications (for a total freezing time of 328±98 s for each PV) successfully isolated 198 of the total 224 (88%) PVs. The average nadir balloon temperatures were -50.3±6.2 degrees for the RSPV, -49.2±4.9 degree for the LSPV, -44.4± -6.0

Table 1: Clinical Characteristics of Patients Per Study Group

	CBA group (n=56)	CF group (n=56)	P value*
Age (years)	64.3±9.8	63.3±10.9	.6371
Sex ratio (M/F)	35/21	37/19	.6933
Duration of AF (months)	12 (5–36)	24 (6–60)	.3494
Body mass index (kg/m²)	23.8±4.1	24.3±4.3	.4646
AF type			
(Paroxysmal/ Persistent)	46/10	42/14	.3570
Hypertension	26 (46)	29 (52)	.5706
Heart failure	6 (11)	3 (5)	.4898
Diabetes mellitus	12 (21)	6 (11)	.1975
Echocardiographic measures			
Left atrial diameter (mm)	39.2±6.6	39.7±5.4	.6752
LVEF (%)	67.7±9.5	67.4±8.1	.9018
Left atrial volume (mL)	40.4±17.2	46.5±18.9	.0744
CTI ablation	23 (41)	20 (36)	.5600

Values are shown as mean±SD, median and interquartile ranges or n (%) unless otherwise indicated. CBA cryoballoon ablation; CF contact force-based radiofrequency ablation; AF atrial fibrillation; LVEF left ventricular ejection fraction; CTI cavotricuspid isthmus.*per Student t-test, Mann-Whitney U-test, chi-square test, or Fisher's exact test, as appropriate.

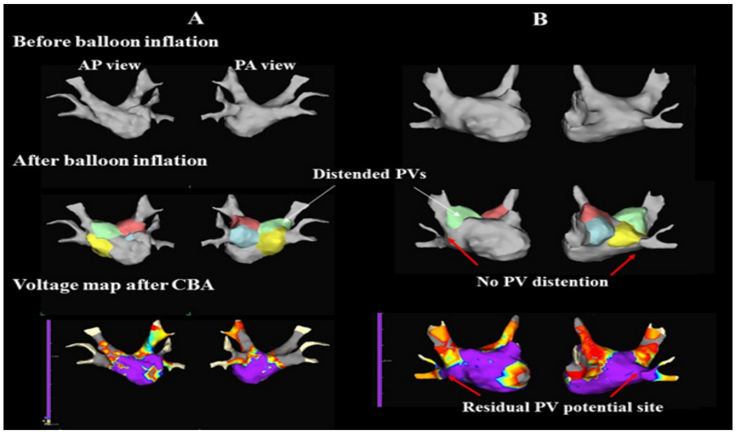

Figure 4: Representative 3D PV distention maps without and with residual PV potentials after cryoballoon ablation. In cases without residual PV potentials (A), balloon inflation concentrically distends the ostia of all 4 PVs (middle panel), resulting in good circumferential ablation lesions, as manifested by a low voltage zone (lower panel). After balloon inflation (B), the ostia of the RSPV, LSPV, and LIPV are evenly distended, but the RIPV ostium is distended mainly in the postero-superior direction (middle panel), resulting in residual PV potentials in the antero-inferior and inferior segments of the RSPV and RIPV (lower panel). Note that the left atrial dimension is larger in the case with residual PV potentials than in the case without it. Abbreviations are as shown in [Figure 3].

degrees for the RIPV, and -42.6±5.1 degrees for the LIPV (P<0.0001 by ANOVA). Complete isolation of all 4 PVs was achieved upon the initial attempt in 38 (68%) of the 56 patients in this group. In the remaining 26 (12%) PVs in 18 (32%) patients, the 3D voltage map and circular mapping catheter recording revealed residual potentials in 28 PV segments (median, 2 [1–2] sites per patient), and these required touch-up ablation to achieve complete PVI. Distribution of the PV segments with a residual potential is shown in [Figure 3]. Fifteen (54%) of the 28 sites with a residual PV potential were located in the inferior region of the RIPV or LIPV In comparison to patients without residual PV potentials, patients with residual PV potentials were younger (59.1±11.5 vs. 66.7±8.0 years, P=0.0053), had a higher body mass index (25.6±4.9 vs. 22.9±3.3 kg/m2, P=0.0166), were more likely to have persistent AF (39% [7/18] vs. 8% [3/38], P=0.0085), and had a greater LA volume (49.1±20.3 vs. 36.3±13.4 mL, P=0.0063) and lower LVEF (63.3±8.7 vs. 69.7±9.3 %, P=0.0175). In contrast, in the CF group, PVI was achieved for all 224 PVs, i.e., for all 56 patients.

After PVI, ATP (30 mg) provoked dormant PV conduction in 9 (4%) of the 224 PVs (in 9 [16%] of the 56 patients) in the CBA group and in 13 (6%) of the 224 PVs (in 8 [14%] of the 56 patients) in the CF group (P=0.3935). The sites of dormant conduction are shown in [Figure 3]. The sites of dormant conduction showed no regional predilection in the CBA group, but in the CF group, sites of dormant conduction were located mainly in the carina regions of the right and left PVs (amounting to 9/14 [64%] PV segments with dormant conduction).

Cryoballoon-Produced PV Distention

As noted above, a PV distention map was created for 21 patients in the CBA group. Representative 3D images of the PV and LA before and after cryoballoon inflation are shown in [Figure 4]. Overall, the inflated balloon stretched the PV ostium surface by 5.2±3.3 mm.

Regionally, the inflated balloon distended the RSPV, LSPV, and RIPV ostia mainly in the postero-superior direction (as defined by the 3 segments showing the greatest distention), but it distended the LIPV ostium in the superior direction. Distention was significantly less in the opposite segments, i.e., in the anterior, antero-inferior, and inferior segments of the RSPV (4.3±3.1 mm vs. 6.5±3.5 mm in the posterior, postero-superior, and superior segments, P=0.0003), LSPV (4.1±2.8 mm vs. 7.3±3.3 mm, P<0.0001), and RIPV (3.0±2.8 mm vs. 6.3±3.0 mm, P<0.0001), and the antero-inferior, inferior, and postero-inferior segments of the LIPV (2.7±2.4 mm vs. 7.4±2.6 mm for the antero-superior, superior, and postero-superior segments, P<0.0001) [Figure 5]. The residual PV potential/dormant PV conduction was found in 25 (3.7%) of the 672 PV segments (21 patients×4PVs×8 PV segments) in the 20 PVs (24% of the 84 PVs), which was strongly associated with contrast leakage before CBA (18 [90%] PVs vs. 5 [8%] in the 64 PVs without it, P<0.0001). The number of residual PV potential/dormant PV conduction sites differed between segments and increased in the following order: 1 (0.6% of the 168 PV segments [21 patients×8 PV segments]), 5 (3.0%), 7 (4.2%), and 12 (7.2%) segments in the LSPV, RSPV, LIPV, and RIPV, respectively (P=0.0084). Importantly, the extent of PV distension was decreased in the PV segments showing residual PV residual PV potential/ dormant PV conduction (2.6±3.4 mm vs. 5.3±3.3 mm, P<0.0001).

Low Voltage and Unexcitable Scar Areas

Representative examples of the PV ablation lesions and ablation points linked to unexcitable tissue are shown in [Figure 2]. We examined 17 RSPVs and 15 LSPVs (2 LSPVs were without pace capture) in 17 CBA group patients and 19 RSPVs and 14 LSPVs (5 LSPV were without capture) in 19 CF group patients. The low voltage area on the 3D LA map was significantly greater in the CBA group patients than in the CF group patients (44.5±15.2% vs. 36.3±5.4%,respectively, P=0.0350), and unexcitable tissue along the ablation line around the PVs was significantly wider in the CBA group patients than in the CF group patients (16.7±5.1 mm

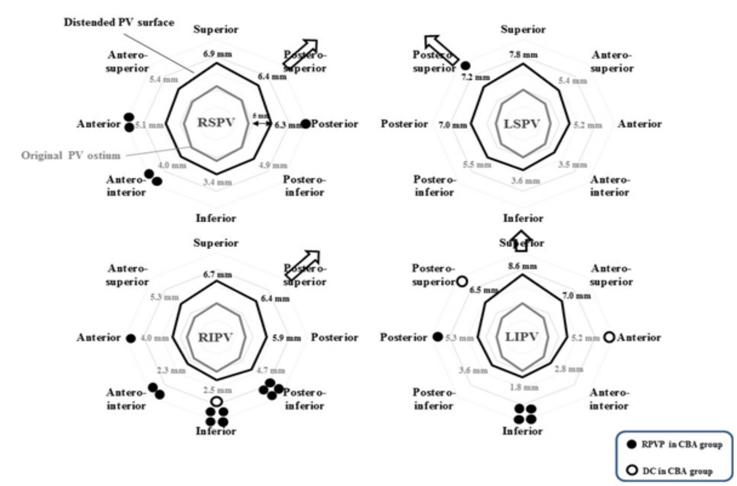

Figure 5: Extent of PV distention after cryoballoon inflation and its relation to residual PV potential/dormant conduction in the various segments of the RSPV, RIPV, LSPV, and LIPV. Black lines indicate the extent of PV distention in the various PV segments, and gray lines indicate the mean diameter of original PV ostium. The PV distention was greatest at 3 of the 8 PV segments, and the measurements are shown in black; the remaining measures of PV distention are shown in gray. Open arrows indicate the main direction of PV distention. Abbreviations are as shown in [Figure 3].

vs. 5.3±2.3 mm, respectively, P<0.0001). Regional differences in unexcitable tissue along the ablation line were noted in the CBA group (P<0.0001 by ANOVA for RSPV and LSPV), but there were no differences between PV segments in the CF group (RSPV; P=0.8194, LSPV: P=0.1183) [Figure 6].

Complications and 1 Year Outcomes

Transient phrenic nerve palsy occurred during RSPV ablation in 3 patients (5%) in the CBA group. No other complication was observed in either group. The AF recurrence rate at a median of 12 months was equivalent at 11% (6/56 patients) in the CBA group and 18% (10/56 patients) in the CF group (P=0.4187).

Discussion

Results of our investigation into the mechanism explaining the success of CBA in treating AF can be summarized as follows: First, the incidence of ATP-provoked PV dormant conduction after CBA was as low as that after CF-based RF ablation, although touch-up ablation was necessary in 32% of patients who underwent CBA. Second, the inflated balloon stretched the PV ostium by 5.2±3.3 mm, but there were regional differences in the PV distension between the LSPV, RSPV, LIPV, and RIPV. Third, the sites of residual potential or dormant conduction were located in PV segments in which distention resulting from inflation of the cryoballoon was moderate rather than extensive. Fourth, the low voltage area resulting from CBA was significantly greater and the unexcitable tissue along the cryoenergy-produced ablation line was significantly wider than those resulting from CF-based RF ablation.

Residual PV Potentials after CBA and Dormant PV Conduction After CBA vs. CF-Based RF Ablation

Previous studies have shown that the efficacy of CBA for paroxysmal AF is similar to that of point-by point RF ablation, but in some patients undergoing CBA, touch-up ablation is required for complete PVI. In our study, touch-up ablation for residual PV potentials was required to complete the PVI in 26 (12%) of the 224 PVs in 18 (32%) of the 56 patients. Touch-up ablation after CBA has been reported for 0–17% of PVs.[15]-[19] In our study, patients with residual PV potentials were relatively young, had a relatively high body mass index and large LA volume, and were likely to have

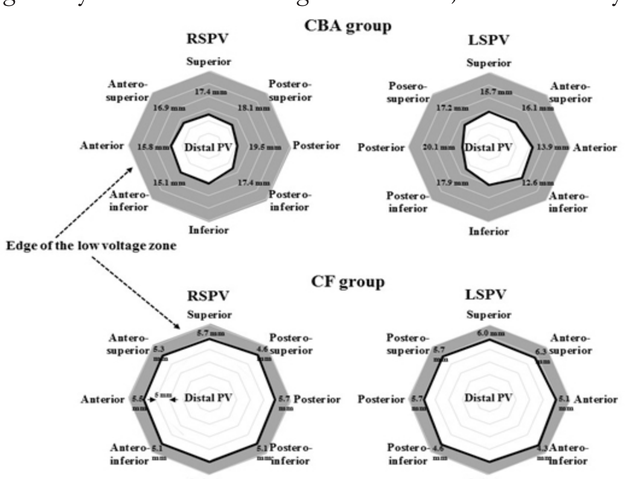

Figure 6: Width of unexcitable ablation lesion in each PV segment of the RSPV and LSPV after CBA and CF-based ablation. Gray areas indicate unexcitable ablation lesions from the edge of the low voltage area on the 3D voltage map. Abbreviations are as shown in [Figure 3].

persistent AF. In addition, we meticulously identified residual PV potentials using 3D voltage map, and we looked for PV potentials not only inside the PV but also in the PV antrum. These patient characteristics and our procedure might account, at least in part, for the incidence of touch-up ablations in our patient series.

The incidence of dormant PV conduction provoked by ATP in our CBA group was lower but statistically comparable to that in our CF group (4% vs. 6% of PVs). The low incidence of dormant PV conduction we encountered after CBA is well in line with previously reported incidences of 2%–8%.[17]-[19] Dormant conduction in our point-by-point RF group was relatively low because we used not only CF but also the VisiTag module, which includes catheter stability information. We reported previously that use of this module reduced the commonly reported incidence of dormant conduction.[12], [20], [21]

Characteristics of Lesions Created by CBA

This study clarified the mechanism explaining good lesions achieved with CBA. Although lesion durability has been documented, a detailed explanation has not been provided.[2]-[6] Adequate CBA occlusion with good balloon-tissue surface contact is important for successful PVI. In theory, extensive, concentric PV distention achieved with the cryoballoon should result in good balloon-tissue surface contact, and we believe that the extensive distention (approximately 7 mm) observed in our study patients was responsible for the creation of ideal ablation lesions around the PV. Nonetheless, our data showed that regional heterogeneity was noted in each PV. The inflated balloon stretched the PV surface in the postero-superior direction in the RSPV, LSPV, RIPV and in the superior direction in the LIPV, resulting in lesser PV distention on the opposite sides. The lesser PV distention was significantly associated with an increased number of residual PV potentials/dormant PV conduction sites.

Similarly, sites requiring touch-up ablation and sites of dormant conduction after CBA are often found in the inferior PVs, especially in the inferior segments of the RIPV.[15],[17]-[19] In the chronic phase, these sites have been reported to be the common sites of PV reconnection.[9],[10],[26] Recently published studies[17]-[19] have suggested that this may be due to malalignment of the cyoballoon, and thus poor balloon-tissue surface contact, in relation to the PV ostium. Therefore, even if PV occlusion by cryoballoon and acute PVI succeed, the lesser PV distention sites can potentially lead to future PV reconnections.

We found that the low voltage area after CBA was significantly larger than that after CF-based RF ablation. Recent studies of CBA have also documented wide and antral ablation lesions.[10],[22]-[24] Nevertheless, the authors assessed only the border line between the ablated and non-ablated regions, and therefore, actual ablated regions within the PV have not been known. We identified the actual ablated regions where PV sleeve tissues were not captured by pacing within the low voltage areas. Unexcitable ablation tissue in the RSPV and LSPV was nearly 3 times longer (16.7 mm) than that (5 mm) achieved by CF-based RF ablation. In fact, the widths of unexcitable ablated tissues that we measured match the reported widths derived from pathological assessment (14±7 mm).[25] Interestingly, PV segments with the widest unexcitable scars were well matched with PV segments showing the greatest PV distention (i.e, the superior, postero-superior, and posterior segments) [Figure 5] and [Figure 6], suggesting that extensive PV distention with good balloon-tissue contact results in wider lesions. These ablated lesion characteristics may explain why CBA-based PVI that persists in the chronic phase was reported in approximately 70% of previously isolated PVs regardless of whether the arrhythmia recurred,[9],[10],[26] and this percentage is significantly higher than the recently published percentage yield of RF ablation.[26]-[29]

Clinical Outcomes

Clinical AF recurrence at a median follow up of 12 months was detected in only 6 (11%) of the 56 patients in our CBA group but in 10 (18%) of the 56 patients in our CF group. Recent studies comparing CF-guided RF ablation with CBA have shown statistical equivalence between the 2 technologies.[7],[8] CBA produces wider lesions which however are not more effective than the more narrow lesions produced by CF-guided RF ablation. This may relate to the fact that even focused lesions may eliminate triggers and that transmural continuous lesions around the PVs may not be necessary in all cases.[9],[10],[26]

Limitations

Our study was limited by the size of the patient groups, considering the fact we performed distension assessments in approximately half of the study patients, because of the tedious and time-consuming nature of the assessment. Nonetheless, the subsequent acute and chronic outcome after CBA are similar to other reports, suggesting that our results will be applicable to analysis of CBA performed for other conditions. Measurement of PV distension after cryoballoon inflation may include an artefact since the measurement of distension was not performed using an absolute geometrical/spatial reference. We did not analyze CBA lesions and PV reconnection sites in the chronic phase. Although some differences can be expected in the chronic phase, the trends should be similar to those in the acute phase.[10], [26]

Conclusions

PV distension produced by cryoballoon inflation appears to be greater in the postero-superior direction than in the antero-inferior direction. Unsuccessful PVI appears to occur when PV distention is relatively inextensive. Overall, CBA lesions appear to be more durable at the posterior and superior aspects of the PV ostia than at the floor of the RIPV. CBA results in wider ablation lesions and unexcitable ablation zones than those resulting from CF-guided RF ablation. This may explain the high efficacy of CBA for paroxysmal AF.

Conflict Of Interests

None.

Disclosures

None.

References

1. Khairy Paul, ChauvetPatrick, LehmannJohn, LambertJean, MacleLaurent, TanguayJean-François, SiroisMartin G, SantoianniDomenic, DubucMarc. Lower incidence of thrombus formation with cryoenergy versus radiofrequency catheter ablation. Circulation. 2003;107 (15):2045–50.
2. Packer Douglas L, KowalRobert C, WheelanKevin R, IrwinJames M, ChampagneJean, GuerraPeter G, DubucMarc, ReddyVivek, NelsonLinda, HolcombRichard G, LehmannJohn W, RuskinJeremy N. Cryoballoon ablation of pulmonary veins for paroxysmal atrial fibrillation: first results of the North American Arctic Front (STOP AF) pivotal trial. J. Am. Coll. Cardiol. 2013;61 (16):1713–23.
3. Fürnkranz Alexander, BordignonStefano, SchmidtBoris, GunawardeneMelanie, Schulte-HahnBritta, UrbanVerena, BodeFrank, NowakBernd, ChunJulian K R. Improved procedural efficacy of pulmonary vein isolation using the novel second-generation cryoballoon. J. Cardiovasc. Electrophysiol. 2013;24 (5):492–7.
4. Chierchia Gian-Battista, Di GiovanniGiacomo, CiconteGiuseppe, de AsmundisCarlo, ConteGiulio, Sieira-MoretJuan, Rodriguez-MañeroMoises, CasadoRuben, BaltogiannisGiannis, NamdarMehdi, SaitohYukio, PaparellaGaetano, MugnaiGiacomo, BrugadaPedro. Second-generation cryoballoon ablation for paroxysmal atrial fibrillation: 1-year follow-up. Europace. 2014;16 (5):639–44.
5. Sport Concussion Assessment Tool 3rd Edition. Br J Sports Med 2013. 2013;47:259–263.
6. Metzner Andreas, ReissmannBruno, RauschPeter, MathewShibu, WohlmuthPeter, TilzRoland, RilligAndreas, LemesChristine, DeissSebastian, HeegerChristian, KamiokaMasashi, LinTina, OuyangFeifan, KuckKarl-Heinz, WissnerErik. One-year clinical outcome after pulmonary vein isolation using the second-generation 28-mm cryoballoon. Circ Arrhythm Electrophysiol. 2014;7 (2):288–92.
7. Squara Fabien, ZhaoAlexandre, MarijonEloi, LatcuDecebal Gabriel, ProvidenciaRui, Di GiovanniGiacomo, JauvertGaël, JourdaFrancois, ChierchiaGian-Battista, De AsmundisCarlo, CiconteGiuseppe, AlonsoChristine, GrimardCaroline, BovedaSerge, CauchemezBruno, SaoudiNadir, BrugadaPedro, AlbenqueJean-Paul, ThomasOlivier. Comparison between radiofrequency with contact force-sensing and second-generation cryoballoon for paroxysmal atrial fibrillation catheter ablation: a multicentre European evaluation. Europace. 2015;17 (5):718–24.
8. Jourda François, ProvidenciaRui, MarijonEloi, BouzemanAbdeslam, HirecheHassiba, KhoueiryZiad, CardinChristelle, CombesNicolas, CombesStéphane, BovedaSerge, AlbenqueJean-Paul. Contact-force guided radiofrequency vs. second-generation balloon cryotherapy for pulmonary vein isolation in patients with paroxysmal atrial fibrillation-a prospective evaluation. Europace. 2015;17 (2):225–31.
9. Heeger Christian-Hendrik, WissnerErik, MathewShibu, DeissSebastian, LemesChristine, RilligAndreas, WohlmuthPeter, ReissmannBruno, TilzRoland Richard, OuyangFeifan, KuckKarl-Heinz, MetznerAndreas. Once Isolated, Always Isolated? Incidence and Characteristics of Pulmonary Vein Reconduction After Second-Generation Cryoballoon-Based Pulmonary Vein Isolation. Circ Arrhythm Electrophysiol. 2015;8 (5):1088–94.
10. Miyazaki Shinsuke, TaniguchiHiroshi, HachiyaHitoshi, NakamuraHiroaki, TakagiTakamitsu, IwasawaJin, HiraoKenzo, IesakaYoshito. Quantitative Analysis of the Isolation Area During the Chronic Phase After a 28-mm Second-Generation Cryoballoon Ablation Demarcated by High-Resolution Electroanatomic Mapping. Circ Arrhythm Electrophysiol. 2016;9 (5).
11. Iso Kazuki, NagashimaKoichi, OkumuraYasuo, WatanabeIchiro, NakaiToshiko, OhkuboKimie, SonodaKazumasa, KogawaRikitake, SasakiNaoko, TakahashiKeiko, KurokawaSayaka, NikaidoMizuki, HirayamaAtsushi. Effect of cryoballoon inflation at the right superior pulmonary vein orifice on phrenic nerve location. Heart Rhythm. 2016;13 (1):28–36.
12. Okumura Yasuo, WatanabeIchiro, IsoKazuki, NagashimaKoichi, SonodaKazumasa, SasakiNaoko, KogawaRikitake, TakahashiKeiko, OhkuboKimie, NakaiToshiko, NakaharaShiro, HoriYuuichi, HirayamaAtsushi. Clinical utility of automated ablation lesion tagging based on catheter stability information (VisiTag Module of the CARTO 3 System) with contact force-time integral during pulmonary vein isolation for atrial fibrillation. J Interv Card Electrophysiol. 2016;47 (2):245–252.
13. Su Wilber, KowalRobert, KowalskiMarcin, MetznerAndreas, SvinarichJ Thomas, WheelanKevin, WangPaul. Best practice guide for cryoballoon ablation in atrial fibrillation: The compilation experience of more than 3000 procedures. Heart Rhythm. 2015;12 (7):1658–66.
14. Iso Kazuki, OkumuraYasuo, NagashimaKoichi. Pulmonary vein distention explaining cryoballoon lesion efficacy. Europace. 2016;18 (2).
15. Kojodjojo Pipin, O'NeillMark D, LimPhang Boon, Malcolm-LawesLouisa, WhinnettZachary I, SalukheTushar V, LintonNicholas W, LefroyDavid,

MasonAnthony, WrightIan, PetersNicholas S, KanagaratnamPrapa, DaviesD Wyn. Pulmonary venous isolation by antral ablation with a large cryoballoon for treatment of paroxysmal and persistent atrial fibrillation: medium-term outcomes and non-randomised comparison with pulmonary venous isolation by radiofrequency ablation. Heart. 2010;96 (17):1379–84.

16. Martins Raphaël P, HamonDavid, CésariOlivier, BehaghelAlbin, BeharNathalie, SellalJean-Marc, DaubertJean-Claude, MaboPhilippe, PavinDominique. Safety and efficacy of a second-generation cryoballoon in the ablation of paroxysmal atrial fibrillation. Heart Rhythm. 2014;11 (3):386–93.
17. Ciconte Giuseppe, ChierchiaGian-Battista, DE AsmundisCarlo, SieiraJuan, ConteGiulio, JuliáJusto, DI GiovanniGiacomo, WautersKristel, BaltogiannisGiannis, SaitohYukio, MugnaiGiacomo, CatanzaritiDomenico, TondoClaudio, BrugadaPedro. Spontaneous and adenosine-induced pulmonary vein reconnection after cryoballoon ablation with the second-generation device. J. Cardiovasc. Electrophysiol. 2014;25 (8):845–51.
18. Miyazaki Shinsuke, TaniguchiHiroshi, NakamuraHiroaki, HachiyaHitoshi, IchiharaNoboru, ArakiMakoto, KuroiAkio, TakagiTakamitsu, IwasawaJin, HiraoKenzo, IesakaYoshito. Adenosine Triphosphate Test After Cryothermal Pulmonary Vein Isolation: Creating Contiguous Lesions Is Essential for Eliminating Dormant Conduction. J. Cardiovasc. Electrophysiol. 2015;26 (10):1069–74.
19. Kumar Narendra, DinhTrang, PhanKevin, TimmermansCarl, PhilippensSuzanne, DassenWillem, VrankenNousjka, PisonLaurent, MaessenJos, CrijnsHarry J. Adenosine testing after second-generation cryoballoon ablation (ATSCA) study improves clinical success rate for atrial fibrillation. Europace. 2015;17 (6):871–6.
20. Park Chan-Il, LehrmannHeiko, KeylCornelius, WeberReinhold, SchiebelingJochen, AllgeierJuergen, SchurrPatrick, ShahAshok, NeumannFranz-Josef, ArentzThomas, JadidiAmir S. Mechanisms of pulmonary vein reconnection after radiofrequency ablation of atrial fibrillation: the deterministic role of contact force and interlesion distance. J. Cardiovasc. Electrophysiol. 2014;25 (7):701–8.
21. Park Chan-Il, LehrmannHeiko, KeylCornelius, WeberReinhold, SchiebelingJochen, AllgeierJuergen, SchurrPatrick, ShahAshok, NeumannFranz-Josef, ArentzThomas, JadidiAmir S. Mechanisms of pulmonary vein reconnection after radiofrequency ablation of atrial fibrillation: the deterministic role of contact force and interlesion distance. J. Cardiovasc. Electrophysiol. 2014;25 (7):701–8.
22. Andrade Jason G, MonirGeorge, PollakScott J, KhairyPaul, DubucMarc, RoyDenis, TalajicMario, DeyellMarc, RivardLéna, ThibaultBernard, GuerraPeter G, NattelStanley, MacleLaurent. Pulmonary vein isolation using "contact force" ablation: the effect on dormant conduction and long-term freedom from recurrent atrial fibrillation--a prospective study. Heart Rhythm. 2014;11 (11):1919–24.
23. Reddy Vivek Y, NeuzilPetr, d'AvilaAndre, LaragyMargaret, MalchanoZachary J, KralovecStepan, KimSteven J, RuskinJeremy N. Balloon catheter ablation to treat paroxysmal atrial fibrillation: what is the level of pulmonary venous isolation?. Heart Rhythm. 2008;5 (3):353–60.
24. Chierchia Gian B, de AsmundisCarlo, SorgenteAntonio, PaparellaGaetano, SarkozyAndrea, Müller-BurriStephan-Andreas, CapulziniLucio, YazakiYoshinao, BrugadaPedro. Anatomical extent of pulmonary vein isolation after cryoballoon ablation for atrial fibrillation: comparison between the 23 and 28 mm balloons. J Cardiovasc Med (Hagerstown). 2011;12 (3):162–6.
25. Kenigsberg David N, MartinNatalia, LimHae W, KowalskiMarcin, EllenbogenKenneth A. Quantification of the cryoablation zone demarcated by pre- and postprocedural electroanatomic mapping in patients with atrial fibrillation using the 28-mm second-generation cryoballoon. Heart Rhythm. 2015;12 (2):283–90.
26. Takami Mitsuru, LehmannH Immo, MisiriJuna, ParkerKay D, SarmientoRay I, JohnsonSusan B, PackerDouglas L. Impact of freezing time and balloon size on the thermodynamics and isolation efficacy during pulmonary vein isolation using the second generation cryoballoon. Circ Arrhythm Electrophysiol. 2015;8 (4):836–45.
27. Miyazaki Shinsuke, TaniguchiHiroshi, HachiyaHitoshi, NakamuraHiroaki, TakagiTakamitsu, HiraoKenzo, IesakaYoshito. Clinical recurrence and electrical pulmonary vein reconnections after second-generation cryoballoon ablation. Heart Rhythm. 2016;13 (9):1852–7.
28. Pratola Claudio, BaldoElisa, NotarstefanoPasquale, ToselliTiziano, FerrariRoberto. Radiofrequency ablation of atrial fibrillation: is the persistence of all intraprocedural targets necessary for long-term maintenance of sinus rhythm?. Circulation. 2008;117 (2):136–43.
29. Jiang Ru-Hong, PoSunny S, TungRoderick, LiuQiang, ShengXia, ZhangZu-Wen, SunYa-Xun, YuLu, ZhangPei, FuGuo-Sheng, JiangChen-Yang. Incidence of pulmonary vein conduction recovery in patients without clinical recurrence after ablation of paroxysmal atrial fibrillation: mechanistic implications. Heart Rhythm. 2014;11 (6):969–76.
30. Neuzil Petr, ReddyVivek Y, KautznerJosef, PetruJan, WichterleDan, ShahDipen, LambertHendrik, YulzariAude, WissnerErik, KuckKarl-Heinz. Electrical reconnection after pulmonary vein isolation is contingent on contact force during initial treatment: results from the EFFICAS I study. Circ Arrhythm Electrophysiol. 2013;6 (2):327–33.